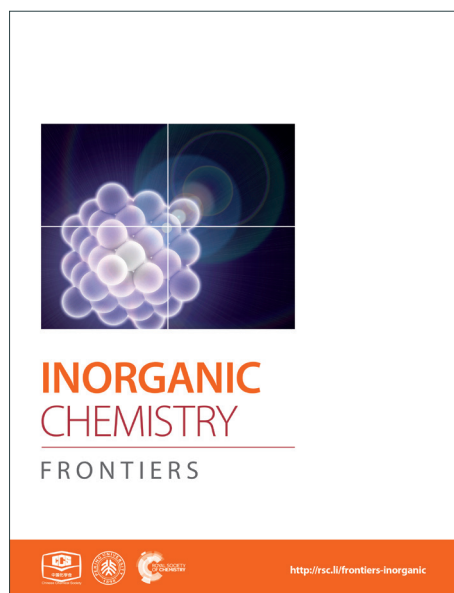
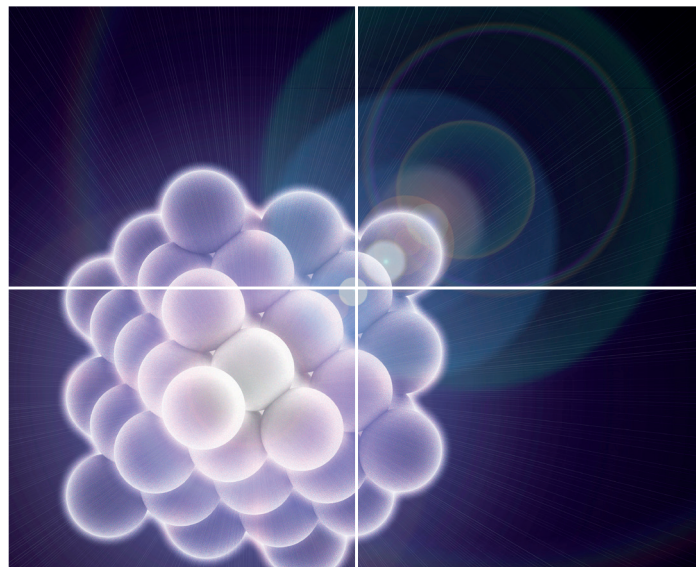


INORGANIC CHEMISTRY

FRONTIERS

Accepted Manuscript



This is an *Accepted Manuscript*, which has been through the Royal Society of Chemistry peer review process and has been accepted for publication.

Accepted Manuscripts are published online shortly after acceptance, before technical editing, formatting and proof reading. Using this free service, authors can make their results available to the community, in citable form, before we publish the edited article. We will replace this *Accepted Manuscript* with the edited and formatted *Advance Article* as soon as it is available.

You can find more information about *Accepted Manuscripts* in the [Information for Authors](#).

Please note that technical editing may introduce minor changes to the text and/or graphics, which may alter content. The journal's standard [Terms & Conditions](#) and the [Ethical guidelines](#) still apply. In no event shall the Royal Society of Chemistry be held responsible for any errors or omissions in this *Accepted Manuscript* or any consequences arising from the use of any information it contains.

Cite this: DOI: 10.1039/c0xx00000x

www.rsc.org/xxxxxx

ARTICLE TYPE

Towards multicomponent MOFs via solvent-free synthesis under conventional oven and microwave assisted heating

Mónica Lanchas,^a Sandra Arcediano,^a Garikoitz Beobide,^{*a} Oscar Castillo,^{*a} Antonio Luque^a and Sonia Pérez-Yáñez^a

5 Received (in XXX, XXX) Xth XXXXXXXXXX 20XX, Accepted Xth XXXXXXXXXX 20XX

DOI: 10.1039/b000000x

Herein we prove the efficiency of the oven heating solvent-free synthesis, based on the acid-base reaction between a metal oxide/hydroxide, adenine (HAde) and monocarboxylic acids, to afford otherwise not accessible new MBioFs of formula $[M_2(\mu_3\text{-Ade})_2(\mu_2\text{-OOC}(\text{CH}_2)_x\text{CH}_3)_2]_n$ expressed as

10 **1_M@monocarboxylate** [M(II): Ni or Zn; monocarboxylate: butanoato (But) and propanoato (Prop)].

Additionally, microwave assisted solvent-free procedure has also been carried out leading to products with a somewhat lower adsorption performance but with the advantage of reducing the reaction times to minute scale and incorporating randomly distributed additional meso/macropores generated during the release of the water vapour byproduct. Both heating techniques provide the resulting products in a

15 monolithic form. The N₂ (77 K) and CO₂ (273 K) adsorption isotherms indicate a great selectivity towards CO₂ for **1_Ni@But** compound. On the other hand, a careful control over the solvent-free

conditions provided good quality single-crystals of three new compounds based on the metal/nucleobase/carboxylate system: $[\text{Zn}_3(\mu_3\text{-Ade})_2(\mu\text{-OOCCH}_3)_4]_n \cdot 3\text{H}_2\text{O}$ (**2**), $[\text{Zn}(\mu\text{-Hypo})(\mu\text{-OOCCH}_3)]_n$ (**3**) (Hypo: hypoxanthinate) and $[\text{Ni}_2(\mu\text{-HAde})_2(\mu\text{-OOCCH}_3)_2(\text{OOCH}_2)(\text{OH}_2)_2] \cdot 2\{(\text{H}_2\text{Ade})(\text{HCOO})\} \cdot 2\text{HCOOH}$ (**4**).

20 Compounds **2** and **3** show lamellar structures without accessible voids. Compound **4** represents an intermediate stage between the initial reagent mixture and the final extended coordination polymers that depicts an insight into the reaction mechanism of the solvent-free approach. It also shows the difficulties on stabilizing the porous structure of **1** when short aliphatic monocarboxylic acids, such as acetic and formic acids, are employed.

25 1. Introduction

During the last decade works focused on metal-organic frameworks (MOFs) have experienced an unremitting increase.¹ They constitute a rapidly growing class of materials due to their permanent porosity, high surface area, large pore volume, and adjustable pore size, distribution and shape.² Moreover, these materials may also exhibit additional properties such as catalytic activity,³ luminescence,⁴ magnetism,⁵ and/or ionic conductivity,⁶ since they benefit from their hybrid metal-organic nature.

There are many reported synthetic routes to obtain MOFs. The most common one implies the reaction between a metal salt and a ligand under solvothermal or microwave assisted solvothermal conditions.⁷ In many cases, the employed solvents are expensive and/or toxic hindering the industrial scale production of MOFs. Thus, green solvents as water and alcohols have gained interest in solvothermal syntheses.⁸ Another option relies on the mechanochemical synthesis, where the reagents are subjected to a vigorous and continuous ball-mill grinding.⁹ The electrochemical synthesis of MOFs in which metal ions are continuously supplied from a metal anode to the reaction media containing the ligand

45 and a protic solvent has attracted the interest of chemical companies.¹⁰ In 2012, it was shown that the solvent-free reaction of a metal oxide or a hydroxide with a diazole or triazole ligand yields zeolitic metal-azolate frameworks when the reaction mixture is heated in an oven for 24-48 hours.¹¹ The key factor for its success relies on the melting of the diazole or triazole ligand under the reaction conditions to provide the necessary mobility for the reaction to progress. More recently, we have proven that this synthetic approach is also extrapolable to carboxylate based MOFs employing low melting temperature metal salts, as the usually employed polycarboxylic acids do not melt before decomposing.¹² In both cases the metal/ligand synthesis ratio fits the amounts required by the formula of the MOF, and as result, the heating of the reagents mixture promotes an acid-base reaction that leads to the desired MOF and to an stoichiometric minor amount of a by-product. The kind of by-product (H₂O, CH₃COOH, HCl, or HNO₃) depends upon the employed metal source, but its volatility at the synthesis temperature favours its removal from the reagents mixture, fostering the reaction progress.

65 The lack of solvent make this novel route more sustainable according to green chemistry principles and it allows to produce

MOFs at lower prices. Moreover, its technical simplicity and ease of scaling makes it highly appealing for the massive MOFs production. However up to now, only examples of two-component MOFs (1 metal + 1 ligand) have been reported. Therefore, in this work we assess the viability of the solvent-free synthesis in a more complex system based on two ligands (adenine/hypoxanthine and a monocarboxylate) and a divalent first row transition cation. The cobalt(II) and copper(II) analogues were synthesized by Rosi and us using solvothermal syntheses and room conditions aqueous synthesis, respectively.¹³ The structure of these compounds is comprised of paddle-wheel shaped centrosymmetric dimeric units, $[M_2(\mu_3\text{-Ade-}\kappa N3:\kappa N7:\kappa N9)_2(\mu_2\text{-OOC}(\text{CH}_2)_x\text{CH}_3\text{-}\kappa O:\kappa O')]_n$ [M^{II} : Cu and Co; x from 0 (acetate) to 5 (heptanoate)], in which two metal(II) atoms are bridged by two adenine ligands coordinated by their N3 and N9 nitrogen atoms and two carboxylic ligands with a $\mu\text{-}\kappa O:\kappa O'$ coordination mode. These units are cross-linked through the apical coordination of the imidazole N7 atom of the adeninato ligands in such a way that each paddle-wheel is linked to four adjacent entities to generate a 4-connected uninodal net with a lv topology and a $(4^2.8^4)$ point symbol, using as a node the dinuclear building unit. The net exhibits a three-dimensional system of intersecting cavities whose effective volume is directly related to the length of the aliphatic chain, which is pointing towards the inner portion of the channels, so that a longer chain implies less free volume.

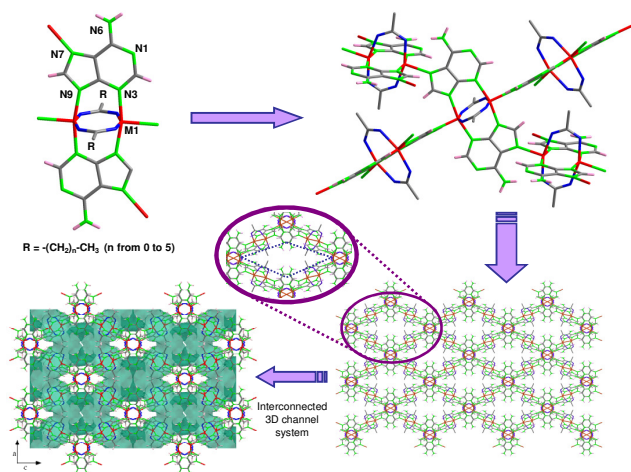


Fig. 1 Porous crystal structure of $[M(\mu_3\text{-Ade})(\mu_2\text{-carboxylate})]_n$ compounds (M being Cu^{2+} or Co^{2+}).

Their crystal structure remains stable upon removal of the solvent molecules showing a relatively great adsorption selectivity towards CO_2 .¹⁴ Spite of the interest of this family of compounds, all the attempts to obtain analogous compounds using other transition metal centers by means of simple aqueous solvent synthesis or under solvothermal conditions were unsuccessful. Therefore, we focus here on the feasibility of the solvent-free route through the synthesis of the otherwise not accessible Zn^{2+} and Ni^{2+} analogues. Additionally, many attempts are also in progress employing different nucleobases to afford similar extended systems. Herein we report a first outcome of using hypoxanthine, a nucleobase closely related to adenine.

We also tested the differences taking place between the conventional oven-heating and microwave assisted heating.

Solvent based microwave-assisted techniques have been widely applied for rapid synthesis of nanoporous materials under hydro/solvothermal conditions.¹⁵ However up to very recently it has not been applied to solvent-free MOF synthesis showing a shortening of the reaction times to few minutes and affording materials with porosity values slightly below those obtained by conventional oven-heating solvent-free procedure and comparable to the results obtained for solvent based synthetic routes.¹²

Experimental section

Materials and methods

All the chemicals used were of analytical grade and used without further purification.

Synthesis

The synthesis of isostructural compounds $[M_2(\mu_3\text{-Ade})_2(\mu_2\text{-OOC}(\text{CH}_2)_x\text{CH}_3)_2]_n$ with code **1_M@monocarboxylate** [M^{II} : Ni or Zn, monocarboxylate: butanoate (But) and propanoate (Prop)] was accomplished using 8 mmol of the corresponding metal oxide/hydroxide (ZnO and $\text{Ni}(\text{OH})_2$) and 8 mmol of adenine that were hand-grinded in a mortar to provide a homogenous reagent mixture, and transferred to a 45 mL Teflon-lined stainless steel autoclave. Later, an excess of propanoic or butanoic acid (27 mmol) was added to account for the amount of carboxylic acid that would go into the vapour phase during the heating process. Afterwards the reaction vessel was placed in a conventional oven with a heating rate of $1^\circ\text{C}/\text{h}$ up to 160°C . Different metal:adenine:carboxylic acid ratios, heating rates and setting temperatures were evaluated but the best results correspond to the conditions above described. Similarly **1_{MW}_M@monocarboxylate** compounds were synthesized in a threaded PTFE reactor and microwave-heated on a household microwave oven (700 W) using reaction times between 6 and 60 minutes.

Compounds $[\text{Zn}_3(\mu_3\text{-Ade})_2(\mu\text{-OOCCH}_3)_4]_n \cdot 3\text{H}_2\text{O}$ (**2**) and $[\text{Zn}(\mu\text{-Hypo})(\mu\text{-OOCCH}_3)]_n$ (**3**) were obtained using again a solvent-free approach on a conventional oven with a heating rate of $1^\circ\text{C}/\text{h}$ up to 160°C , but using an equimolecular ratio of ZnO , adenine and acetic acid ratio for **2** and a ZnO :hypoxanthine:acetic acid ratio of 1:1:5 for **3**. Compound **2** was obtained in a relatively high yield (yield: 88.4% and sample purity: 95.9%), while compound **3** was mixed with some other unknown crystalline phases. Finally, single-crystals of compound $[\text{Ni}_2(\mu\text{-HAde})_2(\mu\text{-OOCH}_2(\text{OOCH})_2(\text{OH}_2)_2)] \cdot 2\{(\text{H}_2\text{Ade})(\text{HCOO})\} \cdot 2\text{HCOOH}$ (**4**), although mixed with some other non-identified compounds, were obtained on reacting $\text{Ni}(\text{OH})_2$, adenine and formic acid on 1:1:3 ratio using a heating rate of $0.5^\circ\text{C}/\text{h}$ up to 120°C . All the products were washed with ethanol to remove unreacted soluble reagents but a small amount of the unreacted $\text{Ni}(\text{OH})_2$ or ZnO is always present in the final product.

Characterization

Elemental analyses (C, H, N) were performed on an Euro EA Elemental Analyzer, whereas the metal content was determined by inductively coupled plasma atomic emission spectrometer (ICP-AES) from Horiba Yobin Yvon Activa. IR spectra (KBr pellets) were recorded on a FTIR 8400S Shimadzu spectrometer

in the 4000-400 cm^{-1} spectral region. Thermal analyses (TG/DTA) were performed on a TA Instruments SDT 2960 thermal analyzer in a synthetic air atmosphere (79% N_2 /21% O_2) with a heating rate of 5 $^\circ\text{C}\cdot\text{min}^{-1}$. Details of the characterization results are gathered on the Supporting Information.

Single-crystal X-ray diffraction data were collected at 100(2) K on an Agilent Technologies SuperNova diffractometer with graphite-monochromated Mo $K\alpha$ radiation ($\lambda = 0.71073 \text{ \AA}$) for **2** and **4** and with Cu $K\alpha$ radiation (1.54185 Å) for **1_Ni@But** and **3**. Data reduction was done with the CrysAlis RED program.¹⁶ Structures of compounds **1_Ni@But** and **2-4** were solved by direct methods using the SIR92 program¹⁷ and refined by full-matrix least-squares on F^2 including all reflections (SHELXL97).¹⁸ The solvent molecules present in the channels of **1_Ni@But** are highly disordered and their contribution to the diffraction pattern has been removed using the SQUEEZE subroutine as implemented in PLATON.¹⁹ All calculations for these structures were performed using the WINGX crystallographic software package.²⁰ Relevant data acquisition

and refinement parameters are gathered in Table 1.

The powder X-ray diffraction (PXRD) patterns were collected on a Phillips X'PERT powder diffractometer with Cu $K\alpha$ radiation ($\lambda = 1.5418 \text{ \AA}$) over the range $5 < 2\theta < 50^\circ$ with a step size of 0.02° and an acquisition time of 2.5 s per step at 25 $^\circ\text{C}$. Indexation of the diffraction profiles was made by means of the FULLPROF program (pattern matching analysis)²¹ on the basis of the space group and cell parameters found for isostructural **1_Ni@But** compound. The unit cell parameters obtained in the final refinement are listed in Table 2. The pattern matching analysis plots are available in the Supporting Information.

The specific surface area was calculated from the adsorption branch in the relative pressure interval from 0.01 to 0.05 using the Brunauer–Emmett–Teller (BET) method,²² while the micropore volume was estimated by fitting the measured N_2 isotherms with the t-plot method.²³ The volumetric carbon dioxide physisorption data were recorded in a Micromeritics ASAP 2020 porosity analyser at 273 K.

Table 1 Crystallographic data and refinement details of compounds **1_Ni@But** and **2-4**.

	1_Ni@But	2	3	4
Empirical formula	$\text{C}_{18}\text{H}_{22}\text{N}_{10}\text{Ni}_2\text{O}_4$	$\text{C}_{18}\text{H}_{26}\text{N}_{10}\text{O}_{11}\text{Zn}_3$	$\text{C}_7\text{H}_6\text{N}_4\text{O}_3\text{Zn}$	$\text{C}_{28}\text{H}_{36}\text{N}_{20}\text{Ni}_2\text{O}_{18}$
Formula weight	559.87	754.60	259.53	1058.19
Crystal system	tetragonal	monoclinic	monoclinic	triclinic
Space group	$I4_1/a$	$P2_1/c$	$P2_1/c$	$P\bar{1}$
a (Å)	15.1973(5)	9.1709(4)	4.7692(2)	7.1579(4)
b (Å)	15.1973(5)	11.7306(4)	10.4912(7)	12.8195(7)
c (Å)	22.1529(8)	12.9958(4)	17.9695(10)	13.0602(7)
α ($^\circ$)	90.0	90.0	90.0	114.763(5)
β ($^\circ$)	90.0	96.400(3)	104.874(5)	100.349(5)
γ ($^\circ$)	90.0	90.0	90.0	100.859(5)
V (Å^3)	5116.4(4)	1389.38(9)	868.97(8)	1022.83(10)
Z	8	2	4	1
$\text{GO}F^a$	1.064	1.041	1.095	1.039
R_{int}	0.0668	0.0708	0.0509	0.0227
Final R indices				
$[I > 2\sigma(I)] R_1^b/wR_2^c$	0.1155/0.2708	0.0600/0.1265	0.0419/0.1131	0.0395/0.0948
All data R_1^b/wR_2^c	0.1204/0.2740	0.0918/0.1404	0.0474/0.1170	0.0543/0.1006
Max/min residual ($e^- \text{Å}^3$)	1.469/-0.731	1.401/-0.620	0.652/-0.659	0.559/-0.372

^a $S = [\sum w(F_o^2 - F_c^2)^2 / (N_{\text{obs}} - N_{\text{param}})]^{1/2}$. ^b $R_1 = \sum ||F_o| - |F_c|| / \sum |F_o|$. ^c $wR_2 = [\sum w(F_o^2 - F_c^2)^2 / \sum wF_o^2]^{1/2}$; $w = 1/[\sigma^2(F_o^2) + (aP)^2 + b]$.

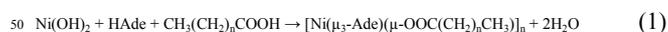
Table 2 Crystallographic data details of compounds **1_Ni@Prop** and **1_Zn@Prop**.

	1_Ni@Prop	1_Zn@Prop
Empirical formula	$\text{C}_{16}\text{H}_{18}\text{N}_{10}\text{Ni}_2\text{O}_4$	$\text{C}_{16}\text{H}_{18}\text{N}_{10}\text{O}_4\text{Zn}_2$
Formula weight	531.77	545.16
Crystal system	tetragonal	tetragonal
Space group	$I4_1/a$	$I4_1/a$
a (Å)	15.581(1)	15.548(1)
c (Å)	21.930(1)	22.630(1)
V (Å^3)	5324(1)	5470(1)

Results and discussion

1_M@monocarboxylate compounds show similar unit cell volume to those of the copper(II) and cobalt(II) analogues (5300-5400 Å^3), except for **1_Ni@But** that shows a significant shrinkage (5116 Å^3). Coordination bond distances are listed in Table 3. We selected $\text{Ni}(\text{OH})_2$ and ZnO to react with the

nucleobase and carboxylic acid because of the greenness of the byproduct generated in the synthesis:



The reaction has been tested at different temperatures. Below 160 $^\circ\text{C}$ the resulting compounds show a lower crystallinity and the reaction yields also decrease. On the other hand, temperatures above 160 $^\circ\text{C}$ provide products with a brownish colour indicative of a partial decomposition of the organic ligands. The heating rate also plays a relevant effect on the crystallinity of the resulting sample and in its particulate size, in such a way that both increase when slower heating is employed. In fact, using a heating rate of 1 $^\circ\text{C}/\text{h}$ crystals of **1_Ni@But** suitable for single-crystal X-ray diffraction characterization were obtained.

Table 3 Selected bond lengths (Å) for compounds **1_Ni@But** and **2-4**.

Compound 1_Ni@But			
Ni1-O1	2.030(7)	Ni1-N17	2.028(6)
Ni1-O2 ⁱ	2.020(7)	Ni1-N19 ⁱⁱⁱ	2.043(7)
Ni1-N13 ⁱⁱ	2.051(7)		
Ni1...Ni1 ⁱ	2.854(3)	Ni1...Ni1 ^{iv}	5.951(2)
Compound 2			
Zn1-O1	2.146(4)	Zn2-O2	1.957(4)
Zn1-O3	2.196(4)	Zn2-O3	1.963(4)
Zn1-N9 ⁱ	2.052(5)	Zn2-N3 ⁱⁱ	2.046(5)
		Zn2-N7	1.994(4)
Zn1...Zn2	3.3734(6)	Zn1...Zn2 ⁱⁱ	5.9415(7)
Compound 3			
Zn1-O1	1.991(2)	Zn1-N7	1.970(3)
Zn1-O2 ⁱ	1.977(2)	Zn1-N9 ⁱⁱ	1.988(2)
Zn1...Zn1 ⁱⁱ	5.8479(5)	Zn1...Zn1 ⁱⁱⁱ	4.7692(2)
Compound 4			
Ni1-O1	2.072(2)	Ni1-O1w	2.064(2)
Ni1-O1 ⁱ	2.066(2)	Ni1-N13	2.123(2)
Ni1-O3	2.025(2)	Ni1-N19 ⁱ	2.123(2)
Ni1...Ni1 ⁱ	3.0218(7)		

^a Symmetry codes for **1_Ni@But**: i) -x+2, -y-1, -z-1; ii) y+3/4, -x+3/4, z-1/4; iii) -y+5/4, x-3/4, -z+1/4; iv) y+3/4, -x+5/4, -z+1/4; for **2**: i) -x+1, y+1/2, -z+1/2; ii) x, -y+1/2, z+1/2; for **3**: i) x-1, y, z; ii) -x+1, y+1/2, -z+1/2; iii) x-1, y, z; for **4**: i) -x+2, -y+2, -z+1.

The same compounds were also synthesized applying a microwave assisted heating solvent-free procedure that allowed to reduce the synthesis time from days to just few minutes. In general, the powder X-ray diffraction patterns of these samples show slightly less intense and broader peaks that those obtained from the conventional oven-heating procedure. Therefore, the crystallinity of the obtained samples is lower than that corresponding to the extended time oven-heating ones but the lowering of crystallinity is less than it would be expected from such a great reaction time reduction. For this experiment a household microwave oven has been used that do not provide control on the temperature but only on the microwave power outsource. The time required to complete the reaction depends on the microwave power changing from 6 to 60 min for *ca.* 4 g batches. The microwave power supply plays also a significant role on the crystallinity and adsorptive properties of the resulting samples as the crystallinity improves on using a lower microwave radiation output and, as a consequence, more extended reaction times. However, the use of very low microwave powers does not provide temperatures high enough to promote the reaction and negligible yields are achieved. The optimal conditions have been found to be around 50% of the maximum microwave output (reaction time: 12 min).

Another relevant aspect of this solvent-free approach, both for conventional oven or microwave assisted heating, is the shaping of the resulting products, that appear in the form of robust monolithic blocks adopting the shape of the reaction vessel. Additionally, due to the nature of the reaction, a simple acid-base neutralization that involves the generation of water as byproduct, the resulting monolith contains interconnected meso- and macropores generated during the release of water vapour. This feature provides a final product in which we can distinguish pores

in the micropore regime, due to the ordered structure of the MBioF, and meso/macropores randomly generated during the texturing of the sample under the synthesis conditions. This phenomenon is more notorious in the microwave assisted heating samples (Fig. 2). The robustness of the monolith can be inferred from the weight that it can stand, at least 200 times its mass. It is worth to mention that nowadays there is a great interest in developing hierarchically ordered porous materials²⁴ and also on developing techniques for shaping²⁵ these materials. This synthetic route affords an easy and simple single-step solution to both issues.

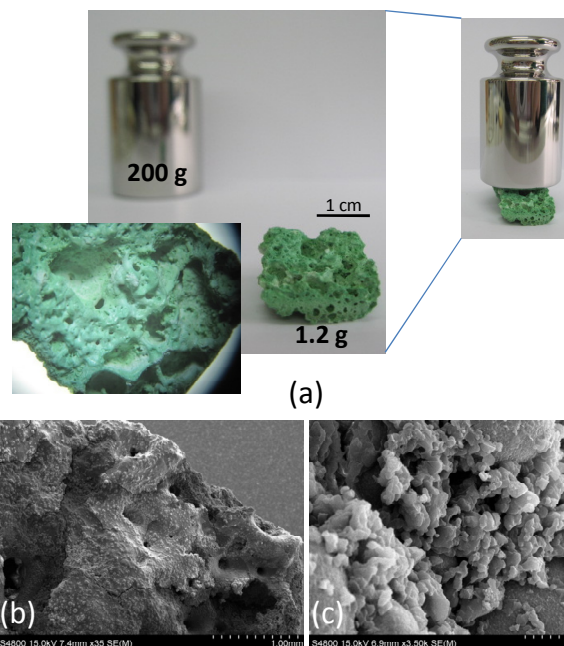


Fig. 2 (a) Monolith of **1_{MW}_Ni@Prop** obtained using microwave assisted heating with an apparent density of 0.35 g/cm³. (b and c) SEM images of the same monolith showing the macroporous texture of the material.

The N₂ and CO₂ adsorption isotherms of these compounds measured at 77 and 273 K (Fig. 3 and Table 4) respectively show that **1_Ni@But** does not adsorb N₂ but it does adsorb CO₂ making this compound a very selective material for the capture of CO₂. This selectivity towards CO₂ was previously described for both Cu²⁺ and Co²⁺ butanoate analogues but it was not so great as to completely avoid the N₂ adsorption at 77 K. The CO₂ adsorption capacity of **1_{MW}_Ni@But** is strongly reduced but conclusions cannot be extrapolated from this fact because the purity of this sample is relatively low. The propanoate analogues adsorb both N₂ and CO₂ but it becomes clear that the performance of the oven-heating samples is better than that of the microwave assisted heating ones. Another interesting feature of the dinitrogen isotherms of the microwave assisted samples is the exponential increase taking place above P/P₀ = 0.8-0.9, which correspond to capillary filling of the microstructural pores greater than 20-30 nm arising from the sample texturization. Similar but less pronounced effect is also found in the oven-heating samples, probably because the more prolonged reaction times promote a less abrupt release of the water vapour.

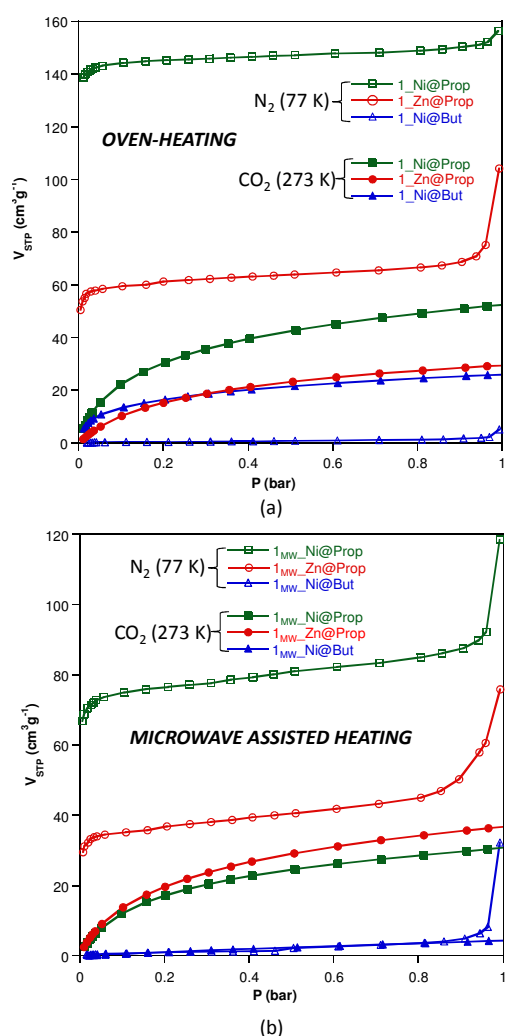
Cite this: DOI: 10.1039/c0xx00000x

www.rsc.org/xxxxxx

ARTICLE TYPE

Table 4 Synthetic results and porosity properties of compounds **1**_M@monocarboxylate.

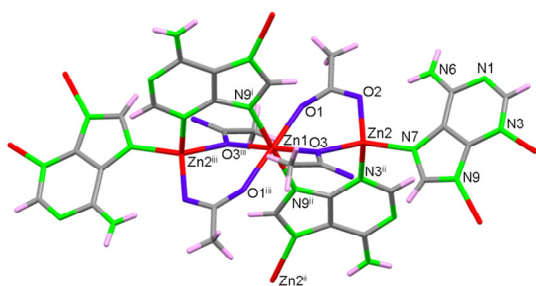
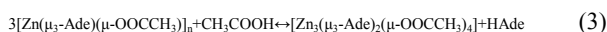
Oven heating (1°C h ⁻¹ , 160°C)							
	Yield (%)	Purity (%)	BET ^a (m ² g ⁻¹)	V _{STP} (N ₂ , P/P ₀ : 0.15) (cm ³ ·g ⁻¹)	V _{STP} (CO ₂ , 1bar) (cm ³ ·g ⁻¹)	V _{micro} (cm ³ ·g ⁻¹)	V _{meso/macro} (cm ³ ·g ⁻¹)
1 _{Ni} @But	98.2	99.4	1	0.4	26.1	0.000	0.007
1 _{Zn} @But	<10	--	--	--	--	--	--
1 _{Ni} @Prop	97.3	99.0	601	144.7	52.6	0.218	0.242
1 _{Zn} @Prop	96.5	98.9	232	60.0	29.6	0.086	0.161
Microwave heating (power output: 50%, 12 min)							
1 _{MW} _{Ni} @But	58.8	88.2	3	0.86	4.6	0.000	0.008
1 _{MW} _{Zn} @But	<10	--	--	--	--	--	--
1 _{MW} _{Ni} @Prop	94.0	97.8	307	75.9	31.9	0.103	0.183
1 _{MW} _{Zn} @Prop	99.2	99.8	146	35.8	36.9	0.044	0.117

^a BET area estimated from the N₂ adsorption isotherm at 77 K.Fig. 3 N₂ (77 K) and CO₂ (273 K) adsorption isotherms of compounds **1**_M@monocarboxylate (a) and **1**_{MW}_M@monocarboxylate (b).

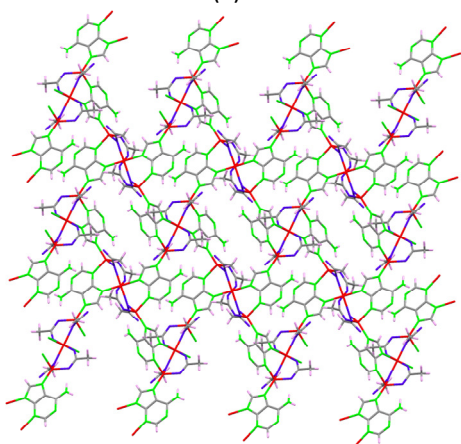
As previously stated, the solvent-free synthetic procedure allowed to obtain the propanoate and butanoate analogues but surprisingly these synthetic conditions did not provide the expected acetate analogue but a non-porous new compound **2** with [Zn₃(μ₃-Ade)₂(μ-OOCCH₃)₄]_n·3H₂O formula is obtained at 160°C. It presents a 2D coordination network composed of linear trimeric [Zn₃(μ-Ade-κN3:κN9)₂(μ-OOCCH₃-κO:κO')₂(μ-OOCCH₃-κO:κO)₂] units (Fig. 4) that are further crosslinked among them through the adeninato ligands. Inside the trimeric entity there are two crystallographically independent metal centers. Zn1, placed in the middle of the trimer, presents a *trans*-N₂O₄ octahedral coordination environment and Zn2, located at both edges, shows a N₂O₂ tetrahedral coordination environment. Inside the trimeric entity, adjacent metal centers are triply bridged by an adeninato ligand with a μ-κN3:κN9 coordination mode and two acetate anions showing different coordination modes, μ-κO:κO' and μ-κO:κO. The adeninate anion, apart from acting as μ-κN3:κN9 bridging ligand inside the trimeric unit, also employs its N7 position to coordinate to a third zinc(II) atom placed at the edge of an adjacent trinuclear entity adopting therefore a μ₃-κN3:κN7:κN9 bridging mode. Interestingly, this is the same bridging mode that it adopts in compounds **1**_M@monocarboxylate. The connectivity array generated makes every trimeric unit to be bonded to four adjacent ones providing a herringbone 2D network that spreads in the (1 0 0) plane. Despite the adeninate anion has its N3, N7 and N9 positions involved in the coordination network, its Watson-Crick face (N1/N6 positions) is exposed outwards the 2D sheet being responsible of the supramolecular assembly of these sheets by means of complementary hydrogen bonding among the adeninates of adjacent sheets.

However upon increasing the ratio of adenine towards the metal and the acetic acid a mixture of compounds **1**_{Zn}@Ace and **2** is achieved (Fig. 5). Unfortunately we have not found the synthetic conditions that could afford **1**_{Zn}@Ace in a pure form but it provides some clues about the equilibrium between both

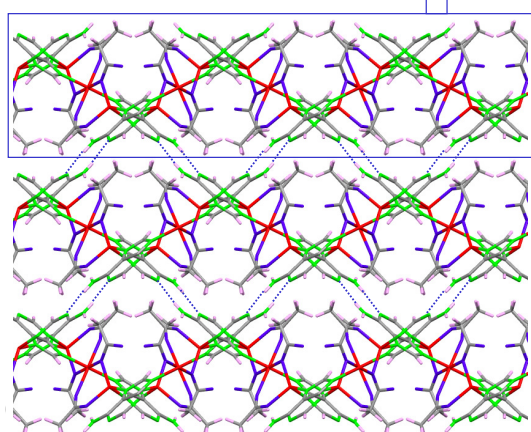
compounds. Based on the equilibrium reaction between compounds **1_Zn@Ace** and **2** (reaction 3) it is easy to understand that an excess of adenine helps displacing equilibrium towards **1_Zn@Ace** as it presents a higher Ade/Zn ratio in its formula. Apart from that it becomes obvious that the aliphatic tails of the butanoate and propanoate bridging ligands play a templating effect helping to stabilize the channel structure, avoiding in this way the growth of a compound analogous to **2**. In fact during the synthesis of the copper(II) analogues in aqueous solution lower amounts of the monocarboxylic aliphatic acids were required as the aliphatic tail increases, supporting also the templating role of the aliphatic chain.



(a)



(b)



(c)

Fig. 4 Trinuclear building units (a) crosslinked by means of μ_3 -adeninato ligands to afford 2D complex sheets (b) that are piled up by means of complementary hydrogen-bonding between the Watson-Crick faces of the adenine in compound **2** (c).

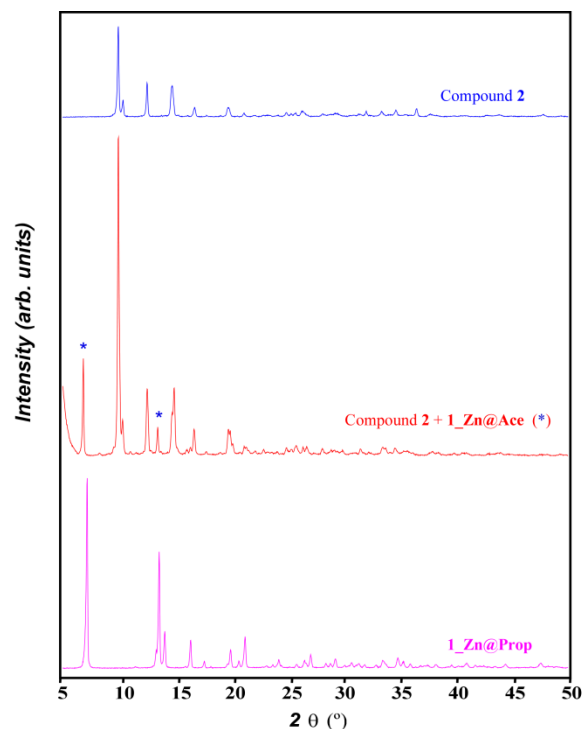


Fig. 5 XRPD pattern of the product resulting from the reaction of ZnO, adenine and acetic acid in a 1:2:1 ratio by slowly heating up to 160°C (1°C/h) and that of compounds **1_Zn@Prop** and **2**.

Performing the same synthesis as for **2** but using hypoxanthine instead of adenine, compound **3** with formula $[\text{Zn}(\mu\text{-Hypo})(\mu\text{-OOCCH}_3)_n]_n$ (Hypo: hypoxanthinate) is achieved. The crystal structure is comprised of tetrahedral Zn(II) metal centers that are bridged by two hypoxanthinate ligands using the imidazolic N7 and N9 positions and by two acetate anions that adopt a syn-anti bridging mode (Fig. 6). Although hypoxanthine behaves mostly as monodentate ligand, it also can act as bidentate bridging ligand (usually as $\mu\text{-N7,N9}$ or $\mu\text{-N3,N9}$) or even as tetradentate ligand. The $\mu\text{-N7,N9}$ coordination mode, that appears in compound **3**, is more frequent than the $\mu\text{-N3,N9}$ mode that commonly appears in paddle-wheel shaped entities.²⁶ This connectivity among the metal centers provides a corrugated 2D structure at which the hypoxanthinate, in its ketonic tautomeric form with the hydrogen atom attached to N1, exposes the O6/N1 face outwards the sheets. Such arrangement allows the piling up of the sheets by means of hydrogen bonding interactions between the hypoxanthinate moieties. As in compound **2**, this new crystal structure does not provide any accessible void.

Crystals of compound **4**, $[\text{Ni}_2(\mu\text{-HAde})_2(\mu\text{-OOCH}_2)(\text{OOCH}_2)(\text{OH}_2)_2] \cdot 2\{(\text{H}_2\text{Ade})(\text{HCOO})\} \cdot 2\text{HCOOH}$, were obtained at significantly lower temperature (120°C) and its crystal structure can be considered as a frozen intermediate structure on the road towards more extended structures in which the acid-base neutralization reaction has been completed. It is comprised of centrosymmetric isolated Ni(II) dimers in which two neutral adenines ($\mu\text{-}\kappa\text{N3}:\kappa\text{N9}$) and two formate anions ($\mu\text{-}\kappa\text{O}:\kappa\text{O}$) acts as bridging ligands to afford an overall paddle-wheel shaped entity (Fig. 7). An additional formate and a water molecule complete the octahedral coordination environment around the Ni(II) metal centers. The Watson-Crick faces of the coordinated adenines belonging to adjacent dimeric entities self recognize to generate

supramolecular chains. Non coordinated formate anions, non-deprotonated formic acid molecules and protonated adeninium cations also cocrystallize with the dimeric entities establishing a complex network of hydrogen bonding interactions. The presence of neutral and protonated adenines altogether with formate and formic acid clearly indicates that this compound is generated at the beginning of the acid-base reaction among $\text{Ni}(\text{OH})_2$, adenine and formic acid. The relatively low temperatures employed in the synthesis has allowed its isolation. Another data that reinforces this interpretation is that only few crystals of this compound were obtained in a mixture of different polycrystalline and amorphous phases, as evidenced from the powder X-ray diffraction data.

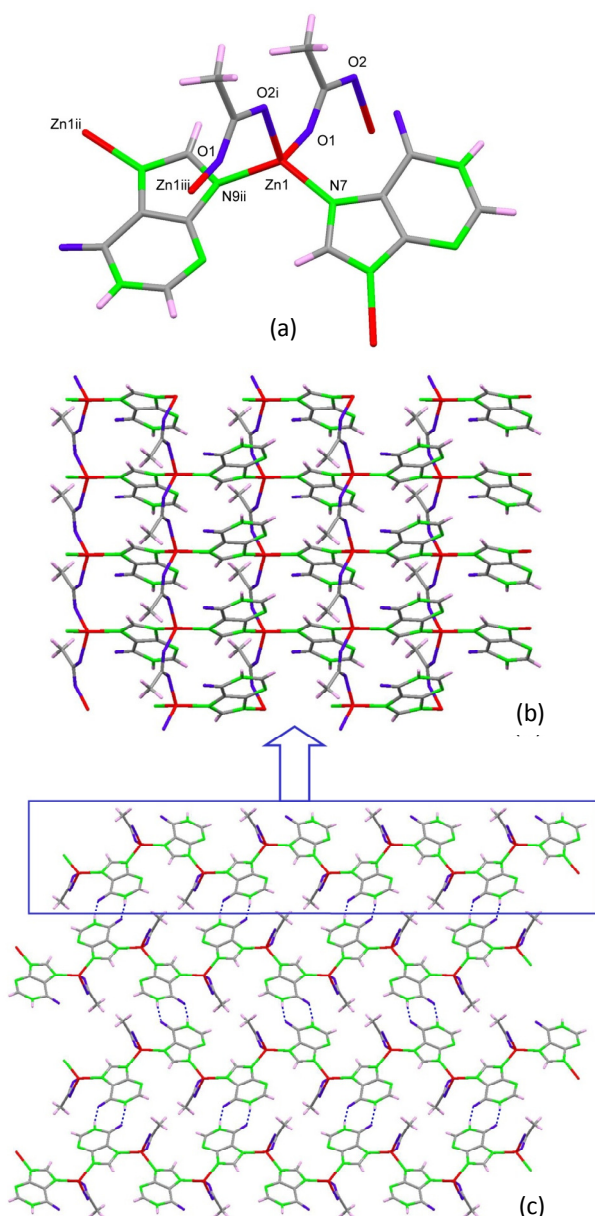


Fig. 6 Coordination environment (a) and 2D complex sheets (b) piled up by means of complementary hydrogen-bonding between the hypoxanthinate ligands (c) in compound 3.

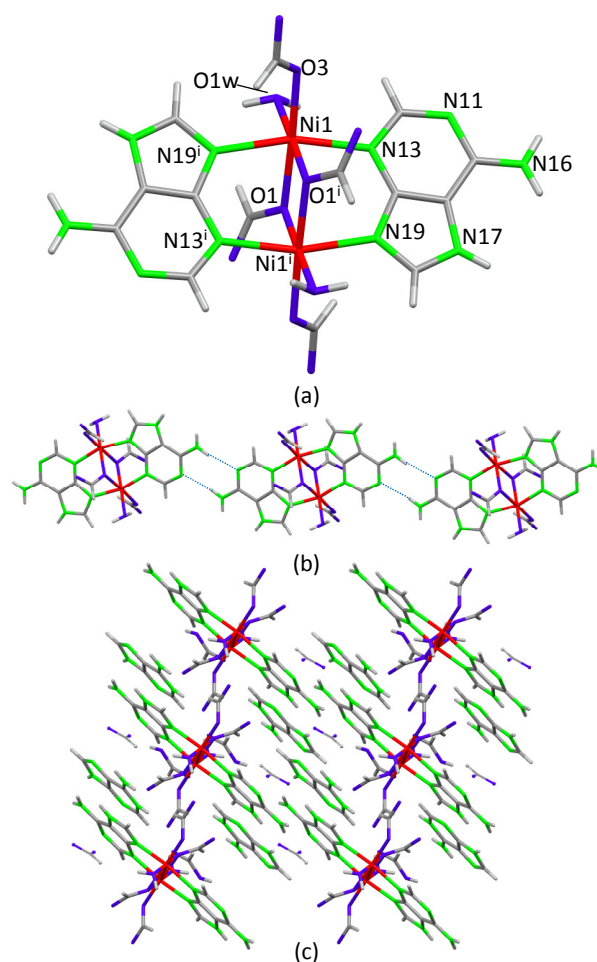


Fig. 7 Dimeric entity (a) and supramolecular dimeric chains (b) assembled together by an extense hydrogen-bonding network involving the cocrystallizing adeninium, formate and formic acid molecules (c) in compound 4.

Conclusions

In this contribution we assess, for the first time, the viability of the solvent-free route by conventional oven heating and by microwave assisted heating to obtain three-component MOFs. There have been synthesized, based on the acid-base reaction between a metal oxide/hydroxide, adenine, and a carboxylic acid, new $[\text{M}_2(\mu_3\text{-Ade-}\kappa\text{N3}:\kappa\text{N7}:\kappa\text{N9})_2(\mu_2\text{-OOC}(\text{CH}_2)_x\text{CH}_3\text{-}\kappa\text{O}:\kappa\text{O}')_2]_n$ MBioFs [where M^{II} : Ni or Zn, x : 1 or 2]. These compounds are not accessible by simple aqueous solvent synthesis or under solvothermal conditions as the previously reported ones for Cu^{II} and Co^{II} analogues. The solvent-free reaction takes place upon heating the reagent mixture by conventional oven-heating but also when using microwave heating. Both heating procedures provide the resulting products in a monolithic form but the microwave heating procedure, although giving lower surface area value, incorporates randomly distributed additional meso/macropores generated during the release of the water vapour byproduct. The adsorptive performance of the resulting product is related to the crystallinity/purity degree of the samples and obviously to the length of the aliphatic chain of the carboxylate ligand that partially occupies the space within the

voids. The longer the chain most selective adsorption towards CO₂ has been observed, as previously reported for the copper(II) and cobalt(II) analogues.^{13,14}

Moreover, three new compounds based on metal/nucleobase/carboxylate system have been characterized by means of single-crystal X-ray diffraction, providing also an evidence of the feasibility of the synthetic procedure to achieve good quality single-crystals. The crystal structure of compounds **2** and **3** correspond to lamellar structures without any accessible void and reflects the difficulties on stabilizing the porous structure of **1** when short aliphatic monocarboxylic acids are employed. On the other hand, compound **4**, containing coordinated formate and adenines together with non-coordinated formate anions, non-deprotonated formic acid molecules and protonated adeninium cations, represents an intermediate stage between the reagent mixture and the extended final coordination polymers. Thus, it depicts an insight into the reaction mechanism of the solvent-free approach.

Finally, we would like to emphasize the greenness of this procedure for MOF synthesis, which is atomically efficient, environmentally friendly and apparently easy to scale up. Moreover, in spite of previous works have analyzed its applications in bicomponent systems, herein we have proven its viability for more complex multi-component systems.

Acknowledgements

This work has been funded by Ministerio de Economía y Competitividad (MAT2013-46502-C2-1-P), Eusko Jaurlaritz/Gobierno Vasco (Grant IT477-10, S-PE13UN016) and UPV/EHU (UFI 11/53, EHUA14/09, postdoctoral fellowship for S.P.Y.). Technical and human support provided by SGIKER (UPV/EHU, MINECO, GV/EJ, ERDF, and ESF) is gratefully acknowledged.

Notes and references

^a Departamento de Química Inorgánica, Universidad del País Vasco, UPV/EHU, Apartado 644, E-48080, Spain. Fax: +34-94601-3500; Tel: +34-94601-5991; E-mail: oscar.castillo@ehu.es

† Electronic Supplementary Information (ESI) available: Details on the syntheses, elemental analyses, IR bands, X-ray powder diffraction analyses, TG curves, and CIF files (CCDC deposition numbers: 1035438-1035441). See DOI: 10.1039/b000000x/

‡ Footnotes should appear here. These might include comments relevant to but not central to the matter under discussion, limited experimental and spectral data, and crystallographic data.

- H. Furukawa, K. E. Cordova, M. O'Keeffe, O. M. Yaghi, *Science*, 2013, **341**, 975.
- (a) N. Stock, S. Biswas, *Chem. Rev.*, 2012, **112**, 933; (b) D. J. Tranchemontagne, J. L. Mendoza-Cortés, M. O'Keeffe, O. M. Yaghi, *Chem. Rev.*, 2009, **38**, 1257.
- (a) M. Kurmoo, *Chem. Soc. Rev.*, 2009, **38**, 1353; (b) C. N. R. Rao, A. K. Cheetham, A. J. Thirumurugan, *Phys.: Condens. Matter.*, 2008, **20**, 083202; (c) A. Dhakshinamoorthy, H. García, *Chem. Soc. Rev.*, 2014, **43**, 5750; (d) J. Liu, L. Chen, H. Cui, J. Zhang, L. Zhang, C.-Y. Su, *Chem. Soc. Rev.*, 2014, **43**, 6011.
- (a) M. D. Allendorf, A. Schwartzberg, V. Stavila, A. A. Talin, *Chem. Eur. J.*, 2011, **17**, 11372; (b) M. Alvaro, E. Carbonell, B. Ferrer, F. X. Labrés i Xamena, H. Garcia, *Chem. Eur. J.*, 2007, **13**, 5106.
- (a) J. Y. Lee, O. K. Farha, J. Roberts, K. A. Scheidt, S. T. Nguyen, J. T. Hupp, *Chem. Soc. Rev.*, 2009, **38**, 1450; (b) E. Coronado, G. Mínguez-Espallargas, *Chem. Soc. Rev.*, 2013, **42**, 1525.

- (a) K. Binnemans, *Chem. Rev.*, 2009, **109**, 4283; (b) K. Kuriki, Y. Koike, Y. Okamoto, *Chem. Rev.*, 2002, **102**, 234; (c) S. V. Elisseva, J. C. G. Bunzli, *New J. Chem.*, 2011, **35**, 1165.
- (a) Y.-R. Lee, J. Kim, W.-S. Ahn, *Korean J. Chem. Eng.*, 2013, **30**, 1667; (b) A. Czaja, E. Leung, N. Trukhan, U. Müller, in *Metal-Organic Frameworks - Applications from Catalysis to Gas Storage*, ed. D. Farrusseng, Wiley-VCH Verlag GmbH & Co. KGaA, 2011, ch. 14, pp. 337-352.
- (a) A. García-Márquez, A. Demessence, A. E. Platero-Prats, D. Heurtaux, P. Horcajada, C. Serre, J.-S. Chang, G. Férey, V. A. de la Peña-O'Shea, C. Boissière, D. Grosso, C. Sanchez, *Eur. J. Inorg. Chem.*, 2012, 5165. (b) A. F. Gross, E. Sherman, J. J. Vajo, *Dalton Trans.*, 2012, **41**, 5458; (c) F.-K. Shieh, S.-C. Wang, S.-Y. Leo, K. C.-W. Wu, *Chem. Eur. J.*, 2013, **19**, 11139; (d) A. C. Kathalikkattil, D.-W., J. Tharun, H.-G. Soek, R. Roshan, D.-W. Park, *Green Chem.*, 2014, **16**, 1607; (e) B. Chen, M. Eddaoudi, T. M. Reineke, J. W. Kampf, M. O'Keeffe, O. M. Yaghi, *J. Am. Chem. Soc.*, 2000, **122**, 11559. (f) Y. Xiao, Y. Cui, Q. Zheng, S. Xiang, G. Qian, B. Chen, *Chem. Commun.*, 2010, **46**, 5503.
- (a) H. Sakamoto, R. Matsuda, S. Kitagawa, *Dalton Trans.*, 2012, **41**, 3956; (b) T. Frišćić, L. Fábíán, *CrystEngComm*, 2009, **11**, 743; (c) S. T. Meek, J. A. Greathouse, M. D. Allendorf, *Adv. Mat.*, 2011, **23**, 249; (d) M. Schlesinger, S. Schulze, M. Hietschold, M. Mehning, *Micropor. Mesopor. Mater.*, 2010, **132**, 121; (e) A. Pichon, A. Lazuen-Garay, S. L. James, *CrystEngComm*, 2006, **8**, 211; (f) M. Klimakow, P. Klobes, A. F. Thünemann, K. Rademann, F. Emmerling, *Chem. Mater.*, 2010, **22**, 5216.
- (a) A. M. Joaristi, J. Juan-Alcañiz, P. Serra-Crespo, F. Kapteijn, J. Gascon, *Cryst. Growth Des.*, 2012, **12**, 3489; (b) U. Mueller, M. Schubert, F. Teich, H. Puetter, K. Schierle-Arndt, J. Pastre, *J. Mater. Chem.*, 2006, **16**, 626; (c) I. Richter, M. Schubert, U. Müller, *PCT Patent*, 2007, **131**, 955.
- (a) M. Lanchas, D. Vallejo-Sánchez, G. Beobide, O. Castillo, A. T. Aguayo, A. Luque, P. Román, *Chem. Commun.*, 2012, **48**, 9930; (b) J.-B. Lin, R.-B. Lin, X.-N. Cheng, J.-P. Zhang, X.-M. Chen, *Chem. Commun.*, 2011, **47**, 9185.
- (a) M. Lanchas, S. Arcediano, A. T. Aguayo, G. Beobide, O. Castillo, J. Cepeda, D. Vallejo-Sánchez, A. Luque, *RSC Advances*, 2014, **4**, 60409.
- (a) J. An, S. J. Geib, N. L. Rosi, *J. Am. Chem. Soc.*, 2010, **132**, 38; (b) S. Pérez-Yáñez, G. Beobide, O. Castillo, J. Cepeda, A. Luque, A. T. Aguayo, P. Román, *Inorg. Chem.*, 2011, **50**, 5330; (c) T. Li, D.-L. Chen, J. E. Sullivan, M. T. Kozlowski, J. K. Johnson, N. L. Rosi, *Chem. Sci.*, 2013, **4**, 1746.
- S. Pérez-Yáñez, G. Beobide, O. Castillo, M. Fisher, F. Hoffmann, M. Fröba, J. Cepeda, A. Luque, *Eur. J. Inorg. Chem.*, 2012, 5921.
- (a) S. H. Jung, J. H. Lee, J. W. Yoon, C. Serre, G. Férey, J. S. Chang, *Adv. Mater.*, 2007, **19**, 121; (b) Y. S. Bae, K. L. Mulfort, H. Frost, P. Ryan, S. Punnathanam, L. J. Broadbelt, J. T. Hupp, R. Q. Snurr, *Langmuir*, 2008, **24**, 8592; (c) N. A. Khan, E. Haque, S. H. Jung, *Phys. Chem. Chem. Phys.*, 2010, **12**, 2625; (d) Z. X. Zhao, X. M. Li, S. S. Huang, Q. B. Xia, Z. Li, *Ind. Eng. Chem. Res.*, 2011, **50**, 2254; (e) E. Haque, S. H. Jung, *Chem. Eng. J.*, 2011, **173**, 866; (f) J. Klinowski, F. A. Almeida Paz, P. Silva, J. Rocha, *Dalton Trans.*, 2011, **40**, 321.
- CrysAlis RED, version 1.171.33.55; Oxford Diffraction: Wroclaw, Poland, 2010.
- A. Altomare, M. Cascarano, C. Giacovazzo, A. Guagliardi, *J. Appl. Crystallogr.*, 1993, **26**, 343.
- G. M. Sheldrick, SHELXL-97, Program for X-ray Crystal Structure Refinement; University of Göttingen: Göttingen, Germany, 1997.
- A. L. Spek, *J. Appl. Crystallogr.*, 2003, **36**, 7.
- L. J. Farrugia, *J. Appl. Crystallogr.*, 1999, **32**, 837.
- (a) J. Rodríguez-Carvajal, FULLPROF, a Program for Rietveld Refinement and Pattern Matching Analysis. Abstracts of the Satellite Meeting on Powder Diffraction of the XVth Congress of the IUCr, Toulouse, France, 1990; p 127. (b) J. Rodríguez-Carvajal, FULLPROF 2000, version 2.5d; Laboratoire Léon Brillouin (CEA-CNRS), Centre d'Études de Saclay, Gif sur Yvette Cedex: France, 2003.

22. S. Brunauer, P. H. Emmet, E. Teller, *J. Am. Chem. Soc.*, 1938, **60**, 309.
23. J. H. de Boer, B. C. Lippens, B. G. Linsen, J. C. P. Broekhoff, A. van den Heeuvel, T. V. Osinga, *J. Colloid Interf. Sci.*, 1966, **21**, 405.
- 5 24. (a) S. Furukawa, J. Reboul, S. Diring, K. Sumida, S. Kitagawa, *Chem. Soc. Rev.*, 2014, **43**, 5700; (b) L. Li, S. Xiang, S. Cao, J. Zhang, G. Ouyang, L. Chen, C.-Y. Su, *Nature Commun.*, 2013, **4**, 1774.
- 10 25. (a) S. Aguado, J. Canivet, D. Farrusseng, *Chem. Commun.*, 2010, **46**, 7999; (b) Y.-R. Lee, J. Kim, W.-S. Ahn, *Korean J. Chem. Eng.*, 2013, **30**, 1667; (c) B. Böhlinger, R. Fischer, M. R. Lohe, M. Rose, S. Kaskel, P. Küsgens, in *Metal-Organic Frameworks – MOF shaping and immobilization*, ed. D. Farrusseng, Wiley-VCH Verlag GmbH & Co. KGaA, 2011, ch. 15, pp. 353-380.
- 15 26. F. H. Allen, *Acta Crystallogr.*, 2002, **B58**, 380 (v. 5.35 – May 2014).